

Article

Thermal Performance of a Cylindrical Lithium-Ion Battery Module Cooled by Two-Phase Refrigerant Circulation

Bichao Lin ^{1,2,3,4} , Jiwen Cen ^{1,2,3} and Fangming Jiang ^{1,2,3,*} 

¹ Laboratory of Advanced Energy Systems, Guangzhou Institute of Energy Conversion, Chinese Academy of Sciences, Guangzhou 510640, China; lbchao95@mail.ustc.edu.cn (B.L.); cenjw@ms.giec.ac.cn (J.C.)

² CAS Key Laboratory of Renewable Energy, Guangzhou 510640, China

³ Guangdong Provincial Key Laboratory of New and Renewable Energy Research and Development, Guangzhou 510640, China

⁴ University of Chinese Academy of Sciences, Beijing 100049, China

* Correspondence: jiangfm@ms.giec.ac.cn; Tel.: +86-20-87057656

Abstract: It is important for the safety and good performance of a Li-ion battery module/pack to have an efficient thermal management system. In this paper, a battery thermal management system with a two-phase refrigerant circulated by a pump was developed. A battery module consisting of 240 18650-type Li-ion batteries was fabricated based on a finned-tube heat-exchanger structure. This structural design offers the potential to reduce the weight of the battery thermal management system. The cooling performance of the battery module was experimentally studied under different charge/discharge C-rates and with different refrigerant circulation pump operation frequencies. The results demonstrated the effectiveness of the cooling system. It was found that the refrigerant-based battery thermal management system could maintain the battery module maximum temperature under 38 °C and the temperature non-uniformity within 2.5 °C for the various operation conditions considered. The experimental results with 0.5 C charging and a US06 drive cycle showed that the thermal management system could reduce the maximum temperature difference in the battery module from an initial value of 4.5 °C to 2.6 °C, and from the initial 1.3 °C to 1.1 °C, respectively. In addition, the variable pump frequency mode was found to be effective at controlling the battery module, functioning at a desirable constant temperature and at the same time minimizing the pump work consumption.

Keywords: battery thermal management; lithium-ion battery safety; refrigerant circulation cooling; electric vehicles



Citation: Lin, B.; Cen, J.; Jiang, F. Thermal Performance of a Cylindrical Lithium-Ion Battery Module Cooled by Two-Phase Refrigerant Circulation. *Energies* **2021**, *14*, 8094. <https://doi.org/10.3390/en14238094>

Academic Editor: Christian Veje

Received: 29 October 2021

Accepted: 29 November 2021

Published: 3 December 2021

Publisher's Note: MDPI stays neutral with regard to jurisdictional claims in published maps and institutional affiliations.



Copyright: © 2021 by the authors. Licensee MDPI, Basel, Switzerland. This article is an open access article distributed under the terms and conditions of the Creative Commons Attribution (CC BY) license (<https://creativecommons.org/licenses/by/4.0/>).

1. Introduction

With the development of high-quality energy storage technologies, as well as environmental awareness and government policy orientation, electric vehicles (EVs) have become the most promising alternative to traditional internal combustion vehicles [1]. The safety, mileage, life cycle, economy, and performance of EVs depend largely on the on-board battery pack. Nowadays, lithium-ion batteries are widely used in EVs due to their state-of-the-art high energy-density and long cycle life [2,3]. The heat generated by the charging or discharging of a lithium-ion battery pack in EVs may cause negative effects or even trigger a thermal runaway if not properly addressed [4–6]. Timely removal of the heat generated, to keep the batteries working in the optimal temperature range during charging/discharging, is a must for maintaining the performance and safety of the battery pack. In addition, the capacity degradation and aging of the battery pack accelerate with the increase of the temperature difference and the working temperature [7]. Research on battery materials, thermal management, and manufacturing technologies can help optimize lithium-ion battery performance. Efficient battery thermal management is currently the most direct and effective method for improving lithium-ion battery performance [8–10].

For EVs, there is a need for a compact and lightweight battery thermal management system (BTMS) [11–13]. The common methods for the thermal management of a lithium-ion battery pack are air cooling, liquid cooling (such as water, glycol, oil, acetone, refrigerant, ammonia, nanofluid, or hydrogel), phase change materials (PCMs), heat pipes, liquid immersion, and some combinations of these [1,14].

Air cooling has attracted much attention, due to its relatively simple structure, lightweight design, and low cost. For a high-power battery energy storage system, as used in EVs, during some aggressive driving cycles and high operating temperatures, a forced-air cooling system can mitigate the temperature rise, but it is likely to cause a serious uneven temperature distribution within the battery pack [15]. A PCM-based passive cooling system can control the temperature rise and improve the temperature uniformity of the battery pack. However, due to the low thermal conductivity of PCM and the intrinsic essence of passive cooling, the combination of PCM and an active cooling system can better meet the cooling requirements of the high-power battery system of EVs [16]. Chen et al. [17] evaluated the performance of active air cooling and passive PCM cooling in terms of battery cycle life and temperature non-uniformity across the battery module. The simulation results showed that the cycle life of the battery module under active air cooling was longer than with PCM cooling, but there was serious temperature non-uniformity. Heat pipe cooling can provide a uniform temperature distribution for the battery pack, due to the superior thermal performance of a heat pipe. However, the high heat generation rate of the pack impedes the wide application of heat pipe BTMSs [18,19].

Liquid has a relatively higher thermal conductivity and specific heat capacity, which can provide sufficient cooling power for the high-power battery packs of EVs, for high-speed cruising modes and fast charging [20]. Many commercial EVs such as the Tesla Model 3, BMW i8, and BYD Song, use a liquid-cooling thermal management system (TMS) for the battery pack. Liquid-cooling BTMSs can be divided into direct and indirect contact schemes, according to whether the battery surface directly contacts the coolant or not. A direct cooling system with mineral oil or silicone oil as the medium has a higher thermal management efficiency, but the parasitic power is larger, and there is a risk of leakage. Therefore, it is more practical to adopt an indirect liquid-cooling thermal management scheme for EV battery packs [15,21]. According to the different control schemes of the system, they can be further divided into active and passive modes. The passive liquid-cooling system has a low efficiency and poor temperature regulation performance, which is only suitable for the cooling of low-power battery packs [22]. Liu et al. [23] used a three-dimensional model to numerically investigate a liquid mini-channel cooling system with various coolants (i.e., water, ethylene glycol, engine oil, and their corresponding nanofluids). It was observed that nanofluids can greatly reduce the maximum temperature of the battery, but cannot effectively improve the temperature uniformity of the battery. Although a liquid-cooling system has a better thermal management capability, it not only also has a more complex structure but increases the weight of the battery system. A hybrid thermal management scheme, based on at least two of the three techniques: PCM, liquid cooling, and heat pipe, combines the advantages of different thermal management strategies and has been widely used. However, the optimal design of a hybrid heat management system is a challenging problem [24]. At present, researchers are still striving to find a high-performance, low-cost method to meet the market demand of BTMSs.

Compared with single-phase forced convection, liquid phase-change absorbs a large amount of the heat generated by the battery, with a lower parasitic power consumption; effectively minimizing the temperature rise in batteries. In addition, the phase change fluids yield a near-isothermal heat transfer, which also minimizes the temperature difference between batteries [25]. A pump-driven two-phase refrigerant BTMS can effectively meet the temperature control requirements of large-capacity battery packs under harsh working conditions. Park et al. [26] investigated the cooling performance of a refrigerant-based active TMS for lithium-ion battery packs in EVs. The cooling performance of their system could be optimized by regulating the refrigerant temperature. In addition, the system

showed excellent cooling performance within the ambient temperature range of 20–40 °C. Hong et al. [27] experimentally studied the performance of using a two-phase refrigerant to directly cool the power batteries of EVs. Due to the more compact structure, the weight of the battery module was only 44% of the liquid-cooling module. The temperature in the battery module exhibited a more uniform distribution. The heat transfer coefficient of the two-phase refrigerant cooling was much higher than that of the single-phase liquid cooling. Under harsh environmental conditions, the two-phase refrigerant cooling was able to control the battery maximum temperature below 45 °C. The battery module with a two-phase refrigerant cooling system had a 16.1% higher battery capacity and 15.0% lower internal resistance compared to a liquid-cooling module. Cen et al. [28] proposed a lithium-ion BTMS, which uses the EVs air conditioning refrigerant to cool the battery module. A basic finned-tube heat exchanger structure and a special aluminum frame were adopted to design the 18,650-type BTMS. The battery module was then integrated into a simulated EV air-conditioning system; two electronic expansion valves were used to automatically control the temperature of the battery module via a self-programmed control software. The experimental results showed that the temperature difference within the battery module was less than 4 °C in the 1.5 C discharge process. Compared with air- and liquid-cooling TMSs, a refrigerant direct cooling BTMS is simpler in structure, which can effectively reduce the weight of the BTMS and improve the energy density and economy of the power system. In addition, the system performs better in controlling the maximum temperature and the temperature difference of the battery pack, and is thus expected to be widely used in EVs [29].

A two-phase refrigerant circulating-cooling battery system is an effective method to make the battery pack operate at the optimal temperature. The cooling system can be directly integrated into the existing EV air conditioning system, and the liquid-refrigerant circulating pump power is usually significantly lower than that required by the air conditioning compressor [30]. Moreover, the system can more effectively absorb the heat generation of batteries than the liquid-coolant used in the secondary cooling system, because of the much larger latent evaporative heat of the refrigerant. Furthermore, the refrigerant-side temperature is relatively stable during the cooling process, so that a very uniform temperature distribution can be achieved in the battery pack.

Compared with single phase liquid-cooling BTMS, a two-phase refrigerant cooling system must be able to withstand the high saturated vapor pressure of the refrigerant. Commonly, a high-pressure system is not lightweight. Special effort is needed in designing a BTMS that can fulfill the requirements of both withstanding high pressure and being light in weight. In addition, in many cases, the heat load is not large enough, and turning on the compressor to cool the battery pack is not energy efficient. Instead, a liquid pump with a smaller power consumption may be sufficient to circulate the refrigerant. However, a two-phase refrigerant cooling BTMS driven by a liquid pump has seldom been reported. In the present work, a R134a-based circulating-cooling BTMS with frequency conversion control was implemented to investigate its thermal management performance. The flow rate of the refrigerant is changeable by adjusting the frequency of the refrigerant circulation pump. The cooling system with finned-tubes was specially designed for a 18,650-type lithium-ion battery module. The thermal behavior of the battery module, cycling under various conditions, were carefully tested and analyzed.

2. Experimental

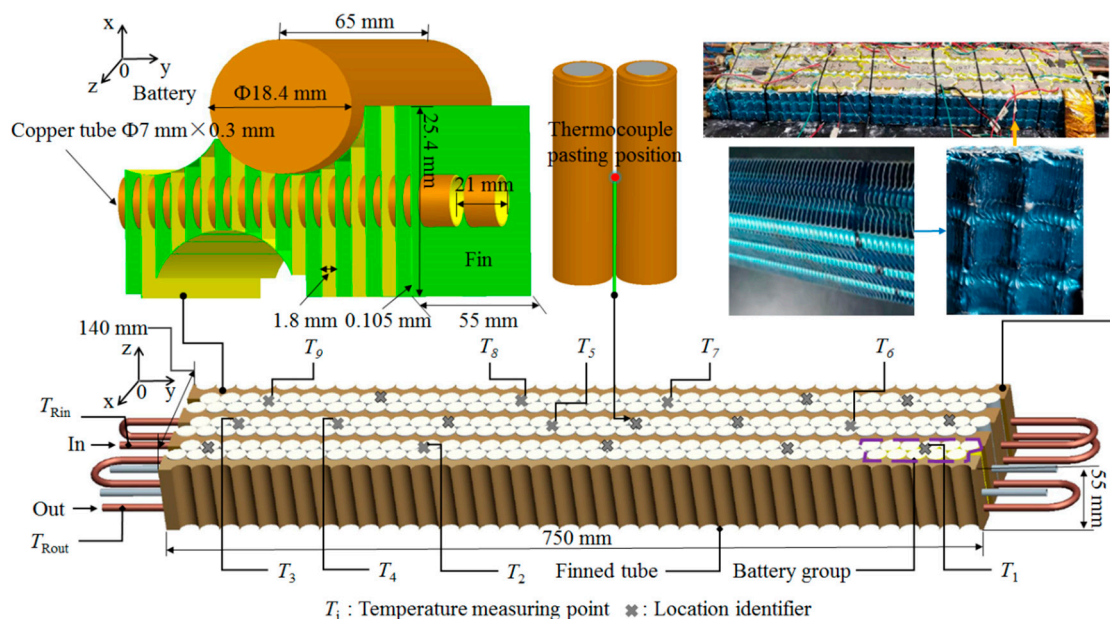
2.1. Battery Module Structure

Commercial 18,650-type lithium-ion batteries with NCM (nickel-cobalt-manganese) cathodes were used to fabricate the battery module. The battery cells have a maximum and minimum operating voltage limits of 4.2 V and 3 V, respectively. The cell parameters are tabulated in Table 1.

Table 1. Parameters of the battery.

Parameter Name	Diameter /mm	Height /mm	Rated Capacity /mA·h	Operating Voltage /V
Value	Φ18.4	65	2600	3.0~4.2

The fabricated experimental battery module, as shown in Figure 1, consists of 240 lithium-ion batteries with ten-cells in parallel (10 P) as a battery group and twenty-four groups in series (24 S). Finned-tubes, commonly used in the heat exchangers of air conditioners, and light in weight and with a high thermal conductivity, were chosen as the cold plate of the battery module. Soft aluminum fins with a length of 25.4 mm, a width of 0.105 mm, and a height of 55 mm, and a copper tube with a diameter of 7 mm (wall thickness of 0.3 mm) were processed together to form a finned-tube, using tube-expanding technology. The spacing between fins is 1.8 mm and that between neighboring tubes is 21 mm. The long module design can improve utilization of the limited space of the vehicle and reduce the components of the battery pack, to improve its energy density. Consequently, the finned-tube was processed into a $760 \times 4 \times 55$ -mm compact finned-tube cold plate and assembled with the 18650-type batteries. The 10P24S battery module also contains K-type thermocouples and a battery protection board, etc. A total of 9 (K-type) thermocouples were attached at a middle-height position on the battery surface, and 2 (K-type) thermocouples were attached on the pipeline surface to measure the inflow and outflow temperatures of the R134a. The uncertainty of temperature measured by the K-type thermocouples was ± 0.3 °C. Geometric dimensions and positions of thermocouples, together with the structure of the battery module are shown in Figure 1.

**Figure 1.** Schematic of the battery module.

2.2. Experimental System

The experimental set-up consisted of a refrigerant circulation system, a battery test system, and a data acquisition system. A schematic of the refrigerant circulation system is shown in Figure 2. The gear pump, the condenser, the battery module, and the refrigerant reservoir constituted the refrigerant circulation system. The refrigerant is driven by a gear pump and has a maximum flow rate of 218 L/h. It absorbs heat from the battery module and dissipates the heat into the water to restore the cooling capacity of the refrigerant. Subsequently, the cooled refrigerant returns back to the reservoir and then proceeds to the

next circulation cycle. The reservoir is located upstream of the pump, to ensure the normal operation of the refrigerant pump. A frequency converter is used to control the flow rate of the refrigerant. By adjusting the frequency of the pump, the flow rate of refrigerant R134a can be changed according to the cooling demand of the battery module. Two pressure transmitters are utilized in the system to measure the R134a inflow and outflow (with respect to the battery module) pressure. The pressure transmitters are products of Nanjing GOVA technology Co. Ltd. and have model type, MB300, with a measurement range of 0–5 MPa and an uncertainty of $\pm 0.2\%$ FS (full scale).

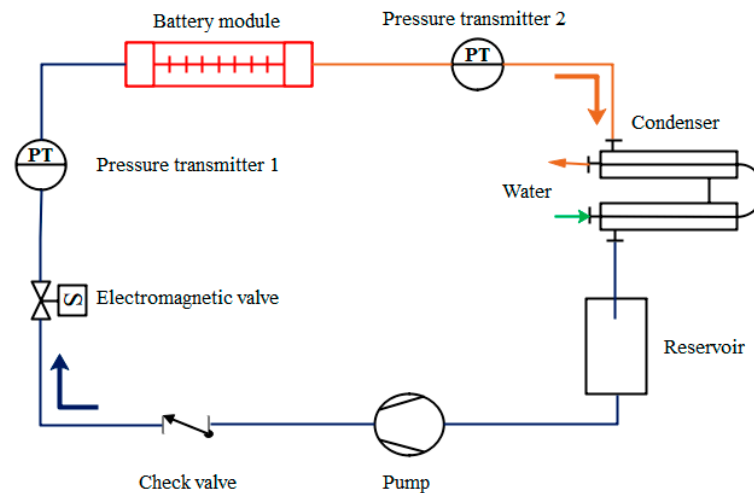


Figure 2. Schematic of the refrigerant circulating battery-cooling system.

Table 2 summarizes the performance parameters of the refrigerant pump and frequency converter used in the refrigerant circulation system. It should be noted that in practice, the refrigerant-circulation battery cooling system is not isolated, but integrated with the EV air conditioning system. The pump of the battery cooling system is set in parallel with the compressor of the EV air conditioning system and they share the same condenser. Under some working conditions, such as low temperature environments and mild charge/discharge rates, to save energy, the compressor could be turned off and only the refrigerant pump need be on to fulfill the requirement of battery thermal management.

Table 2. Performance parameters of the pump and frequency converter.

Pump	Frequency Converter
Power: 120 W	Rated capacity: 1.9 kVA
Flow: 130~218 L/h	Input current: 12.8 A
Head: 90~310 kPa	Rated output current: 5 A

2.3. Experimental Conditions

In the experiments, the battery module was brought to an ambient temperature of 25.5–26.5 °C. The modes of constant current (CC) for battery module discharging and constant current–constant voltage (CC–CV) for charging were used. The cut-off voltage in the discharge processes was 82 V, and the voltage for changing from a constant current into constant voltage operation in the CC–CV charge processes was 100 V. The experiments were carried out by adjusting the frequency of the pump motor to control the temperature and temperature difference of the battery module within the desired range. The thermal performance of the battery module at different charge/discharge rates, under US06 road driving discharge conditions, as well as with large initial temperature differences between batteries were tested. A series of experiments with similar conditions were performed to guarantee the results had adequate repeatability.

3. Results and Analysis

3.1. Constant Pump Frequency Mode

Figure 3 presents the measured temperatures as a function of the state of charge (SOC) during the 0.5 C charge process. When the measured maximum temperature reaches 30.5 °C, the gear pump is engaged, and the refrigerant circulating system starts to cool the battery module. The operating frequency of the pump is 21 Hz. It was found that the temperature of the battery module could be controlled within the desired range of 20–40 °C. Seen from the temperature versus SOC curves in Figure 3, the refrigerant cooling appears to be very effective, the measured temperatures started to decrease upon startup of the pump and a temperature platform of about 26.5 °C quickly appeared, and then the measured temperatures decreased again due to the lowered heat generation as the battery charge process turned to the constant-voltage mode, when SOC was about 0.8. The maximum temperature difference of the battery module during 0.5 C charging was about 1.5 °C

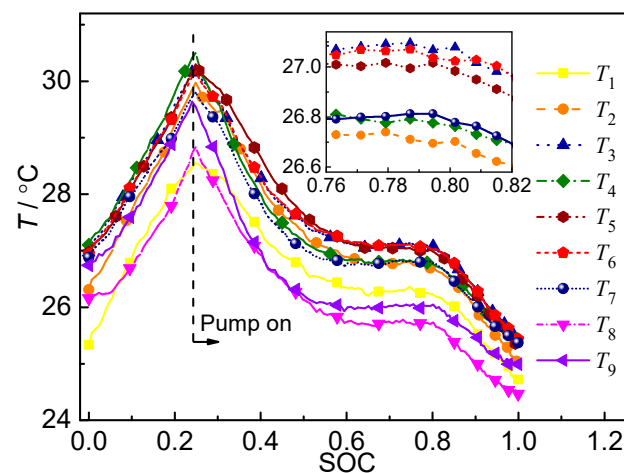


Figure 3. The measured temperatures of the battery module during 0.5 C charging. The pump's frequency is 21 Hz when on.

Figure 4a gives the measured temperatures as a function of depth of discharge (DOD) during the 1 °C discharge process. When the average temperature rises to 30 °C and the maximum temperature reaches 32 °C, the refrigerant circulating system is engaged, and the pump operates at a frequency of 50 Hz. It can be seen from Figure 4a that the temperature of the battery module can be maintained at about 29 °C, and the temperature difference is about 2.0–2.5 °C. A comparison experiment was also carried out, in which the battery module used 1 C discharging, under the same environmental conditions, whereas the battery thermal management system was kept off throughout the process. The maximum temperature measured in the battery module was about 55 °C, and the maximum temperature difference was up to 9.2 °C. The circulating refrigerant cooling effectively controls the temperature rise and reduces the maximum temperature difference in the battery module.

The refrigerant flow experiences a pressure drop when passing the battery module. As shown in Figure 4b, there immediately appears a pressure difference between the two pressure monitoring points upon startup of the pump. The inlet pressure rises and the outlet pressure drops compared with the initial stationary pressure. The pressure difference occurs because of the flow resistance of flow pathways inside the battery module. The refrigerant is always in a two-phase state and the pressure–temperature strictly follow the saturated pressure–temperature relationship of the refrigerant. The pressure drop will cause a corresponding change in the temperature of the refrigerant; the corresponding temperature change of the refrigerant is about 4 °C according to the pressure difference shown in Figure 4b. The higher the temperature difference of the refrigerant between

the inlet and outlet, the larger the temperature non-uniformity that may be caused in the module. Therefore, it is desirable to make the flow resistance small, to improve the thermal management performance.

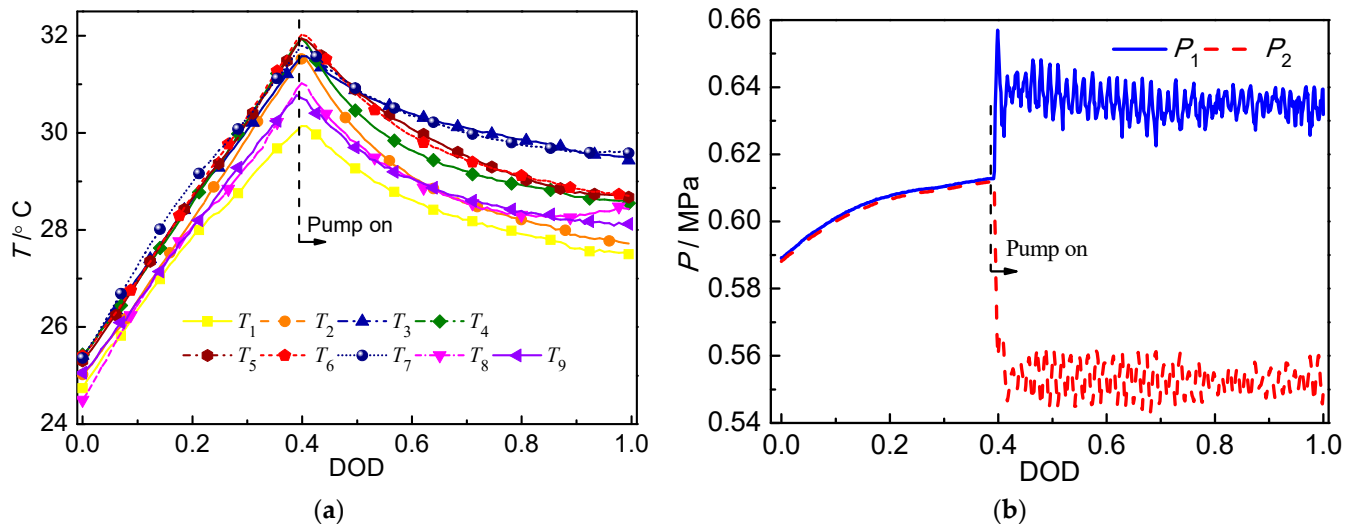


Figure 4. Evolution of (a) the monitored temperatures and (b) the inflow and outflow pressures during 1.0 C discharging. The pump operates at 50 Hz if on.

As seen from Figures 3 and 4a, there always exists some temperature differences among the monitoring points, which may be ascribed to the reasons detailed in the following: (i) Change of refrigerant saturated temperature. Unlike in traditional single-phase liquid-cooling, in which the fluid temperature increases gradually from inlet to outlet, the two-phase refrigerant absorbs heat in the form of latent heat and its temperature is the corresponding saturated temperature with respect to the local fluid pressure. The refrigerant temperature changes little if the pressure difference between inlet and outlet is small. However, due to flow resistance, the inlet pressure must be higher than outlet, then, the corresponding saturated temperature at the inlet is higher than that at the outlet. (ii) Different monitoring points have different heat release conditions. (iii) The batteries may have different heat generation rates. (iv) Some small differences in the initial temperature exist between the batteries. (v) The thermal contact conditions of batteries with the cooling fins or to the thermal couple may be not the same. (vi) The measuring uncertainty of the thermal couples is ± 0.3 K, which is comparable to the temperature difference between the batteries. All these factors caused the seemingly irregular temperature behaviors observed in Figures 3 and 4a.

Figures 3 and 4a also show the lowest temperature appeared at different monitoring points. The most probable reason is that for different charge/discharge rates, different amounts of heat generation lead to different two-phase flow patterns (e.g., flow type, dryness distribution) along the pipeline, causing locally different heat transfer coefficients.

3.2. Variable Pump Frequency Mode

Compared with a constant pump frequency mode, the variable pump frequency mode may lower the pump work consumption without lowering the effectiveness of the refrigerant cooling. To better understand the advantage of variable pump frequency operation, we can consider cases of constant pump frequency, e.g., the case related to Figure 3. The CC–CV charge process generates less heat after it turns to the CV phase; however, the constant pump frequency makes the refrigerant still work at the same cooling intensity, and the battery temperatures are seen to continuously drop. A variable pump frequency mode aims at effective cooling, to keep the battery working in a desirable temperature range, while consuming the least pump work. A pre-test revealed that

the battery module could achieve an approximately constant temperature during 0.9 C discharging if the refrigerant cooling was operated at a constant pump frequency of 50 Hz. As the largest frequency could be just 50 Hz for the pump used in the experimental system, the battery discharge rate had to be smaller than 0.9 C when performing the variable pump frequency experiment.

Figure 5 presents the measured battery temperatures, refrigerant inflow and outflow temperatures as a function of DOD during the 0.6 C discharge process. When the maximum temperature of the battery module rises above 31 °C, the refrigerant circulation cooling system is engaged to cool the battery module. According to the real-time temperature change of the battery module, the operation frequency of the pump was adjusted mechanically, to explore the influence of the variable pump frequency operation mode on the battery module temperature. The pump frequency was lowered from the initial 35 Hz to 30.1 Hz at DOD = 0.82, after which it did not change any more. The regulation of the pump operating frequency is indicated in Figure 5b. The temperature of the battery module, as shown in Figure 5a can be controlled at a constant level during the ending phase of the discharge process. In other words, the variable pump frequency mode effectively and quickly removes the battery heat generated and minimizes the pump work consumption. In a real situation, the pump frequency could be automatically adjusted using an intelligent method, instead of manual operation. As also seen from Figure 5a, during the experimental discharge process, the maximum temperature difference of the battery module was about 2.5 °C.

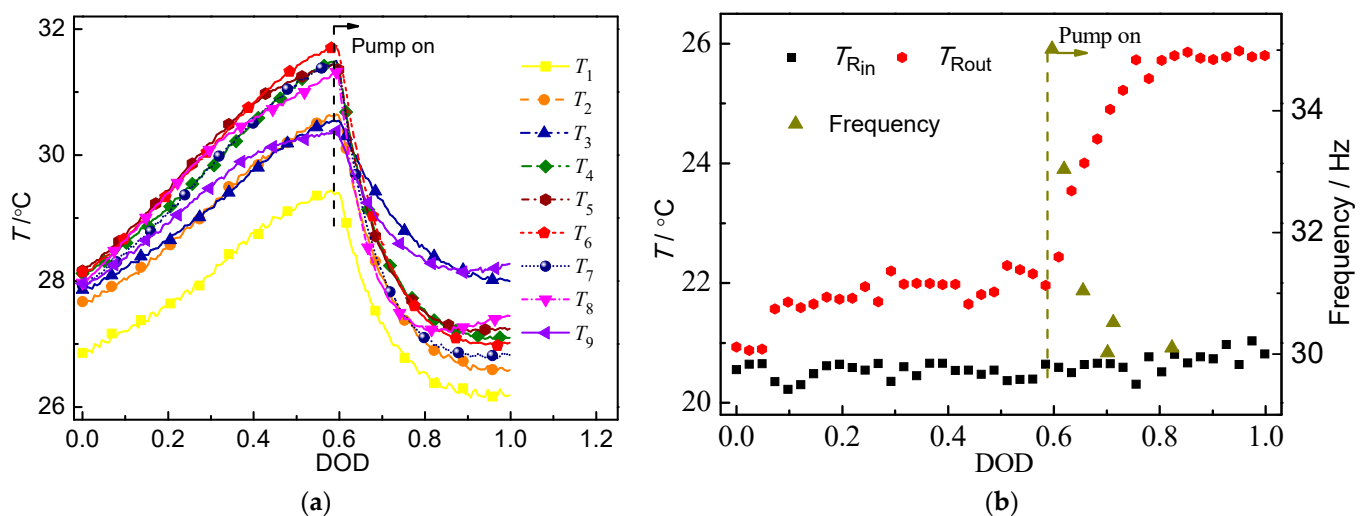


Figure 5. The evolution of (a) battery pack temperature and (b) refrigerant temperature when the battery module was discharging at 0.6 °C, the pump operates in variable frequency mode.

The refrigerant inflow and outflow temperatures given in Figure 5b show that the refrigerant outflow temperature increased with the DOD after the pump was turned on, which is an expected result, as the pump frequency was lowered overall and less refrigerant was fed into the battery module.

3.3. Severe Operation with Large Initial Temperature Difference

To further test the thermal management performance of the refrigerant-cooling system, severe operation conditions with a large initial temperature difference in the battery module were considered. A large initial temperature difference could be produced by intentionally incorrect operation of the refrigerant cooling system, e.g., an inappropriate pump frequency. Figure 6 presents the measured temperatures and refrigerant pressure and inflow/outflow temperatures as a function of SOC during the 0.5 °C charge process. The batteries had large temperature differences initially. Once the maximum battery temperature had risen above 37 °C, the pump started to work at a frequency of 50 Hz, and the refrigerant continuously

cooled the battery module. The experimental results show that the initial maximum temperature difference of the battery module was $4.5\text{ }^{\circ}\text{C}$. During the charging process, the maximum temperature of the battery module rose to above $37\text{ }^{\circ}\text{C}$ at $\text{SOC} \approx 0.35$, which triggered the cooling system. The cooling system could control the temperature of the battery module in the desired temperature range, and the maximum temperature difference was greatly reduced. The region containing the temperature curves of the different batteries was seen to become narrower after the pump was turned on. At the end of the charging process, the temperature difference of the module was reduced by about 42.4% compared to the initial $4.5\text{ }^{\circ}\text{C}$ temperature difference.

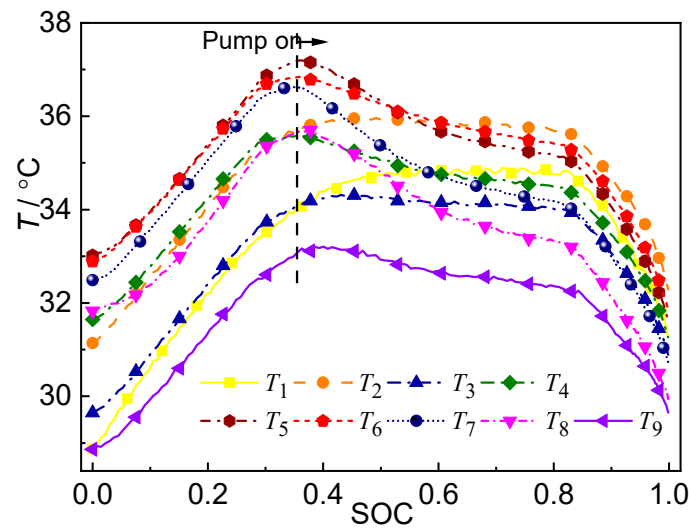


Figure 6. Evolution of the battery pack temperature when the battery module was charging at $0.5\text{ }^{\circ}\text{C}$, the pump runs at 50 Hz with a large initial temperature difference.

3.4. Discharge with Simulated Road Driving Conditions

In the present study, the US06 driving cycle developed by the U.S. Environmental Protection Agency was adopted to verify the cooling performance of the refrigeration circulating cooling system for the battery module in circumstances close to the real road driving conditions. The US06 has a 129.2 km/h maximum speed. The theoretical travel distance is 12.8 km , with a testing time of 596 s . However, the test standard only provides the speed–time curve of the cycle. It is necessary to calculate the power–time curve in order to implement the test cycle of the battery module. The vehicle speed and power in the US06 test are shown in Figure 7.

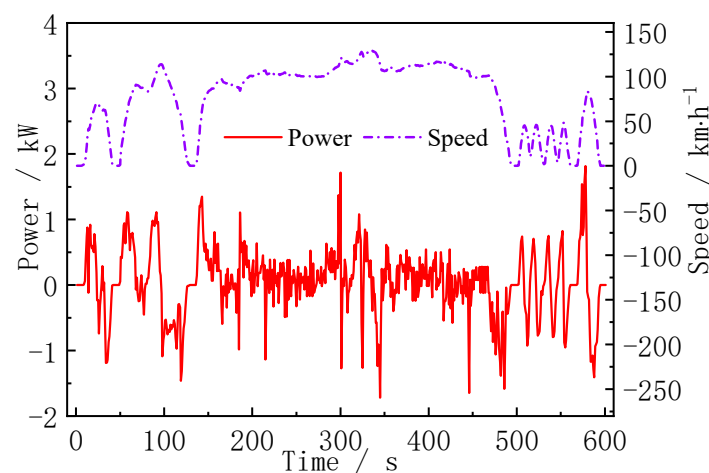


Figure 7. The speed and power of the US06 test process.

The conversion formula is given as follows [26]:

$$P_b = \frac{1}{\eta_T \eta_E} \left(\frac{mgf u_a \cos \alpha}{3600} + \frac{mg u_a \sin \alpha}{3600} + \frac{C_D A u_a^3}{76,140} + \frac{\delta m u_a}{3600} \frac{du}{dt} \right) \quad (1)$$

$$P_c = \frac{V_c Q_c}{V_b Q_b} P_b = \lambda_B P_b \quad (2)$$

where P_b (kW) is the battery pack output power; $\eta_T = 0.95$, the transmission efficiency; $\eta_E = 0.931$, the energy efficiency of the power circuit; $m = 1235$ kg, vehicle mass; $g = 9.8$ m/s², acceleration of gravity; $f = 0.0055$, rolling resistance coefficient; $\alpha = 0$, gradient angle; $A = 1.9$ m², vehicle windward area; $C_D = 0.35$ is the coefficient of air resistance; u (m/s) and u_a (km/h) are speed; $\delta = 1.05$, rotary mass conversion coefficient; P_c , the battery module output power; $V_c = 84$ V and $Q_c = 22$ Ah are the voltage and capacity of the battery module, respectively; $V_b = 375$ V and $Q_b = 53$ Ah are the voltage and capacity of the Tesla Roadster vehicle battery pack, respectively; and λ_B is the battery equivalent coefficient [31].

Figure 8 gives the temporal evolution of the measured temperatures, along with the variation of SOC of the battery module. The ambient temperature of the battery module was about 25.7 °C during the US06 test. The pump was immediately started with the battery module in the simulated conditions. The pump operating frequency was set to 30 Hz. The experimental results show that the refrigerant circulating cooling system could reduce the temperature and temperature difference of the battery module effectively, and its maximum temperature difference under the US06 test was about 1.1 °C lower than the initial 1.3 °C. Since, the average discharge current of the battery module was small due to the stopping and decelerating processes during the driving cycle, the temperature difference was very small throughout the test period, as shown in Figure 8. Therefore, the refrigerant circulating cooling system designed in this work could meet the cooling requirements of the battery pack under the US06 cycle.

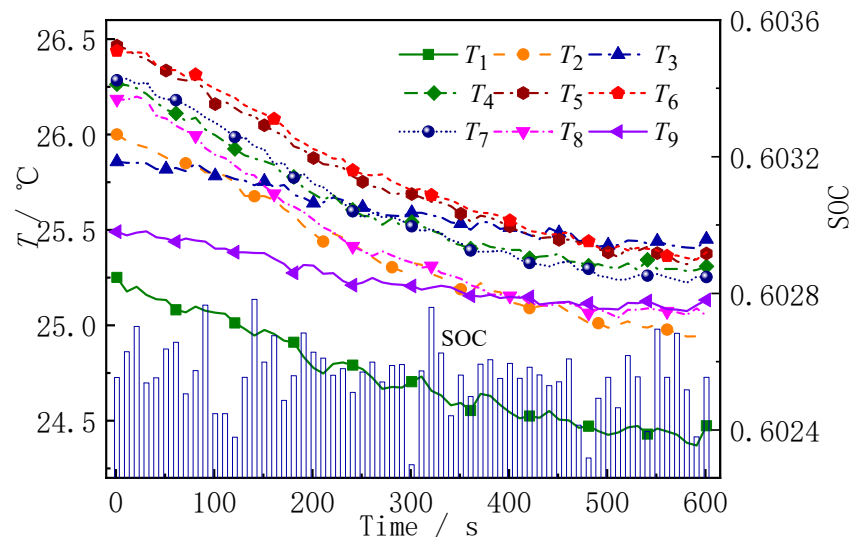


Figure 8. Time evolution of the battery module temperature during the US06 test; the pump operating frequency was 30 Hz.

4. Conclusions

For EV battery packs, it is important to avoid the adverse effects that of out of range peak temperature and temperature non-uniformity could have on thermal safety, power performance, and life cycle. In this study, a refrigerant circulating cooling battery thermal management system with a frequency regulation control, based on the air conditioning system of the EV was designed. In addition, a light-weight finned-tube heat exchanger structure was adopted to produce a compact 10P24S rectangular battery thermal man-

agement module. Temperature control of the refrigerant circulating cooling system was achieved by pump frequency regulation with different charging/discharging rates of the battery module. The experimental results showed that the designed cooling system could meet the cooling requirements of the battery module. The main conclusions are as follows:

- (1) When the battery module was charged and discharged at the C-rates considered, the refrigerant circulating cooling system could maintain the battery module within the optimum temperature range. Compared with the 0.5 °C charge process, the 1 °C discharge process, which generates more heat, showed a greater temperature uniformity. Nevertheless, the temperature difference in the battery module remained about 2.0–2.5 °C during the tested 1 °C discharge process.
- (2) During the tested 0.6 C discharge process, the temperature of the battery module was approximately constant when gradually reducing the pump frequency from the initial 35 Hz to 30.1 Hz.
- (3) In the tested battery charging case with severe working conditions (i.e., a large initial temperature difference), the refrigerant cooling system could effectively control the rise in battery temperature and also reduce the temperature difference.
- (4) The refrigerant circulating battery cooling system could meet the cooling requirements of the battery pack operating under the US06 cycle.

Author Contributions: Conceptualization, J.C. and F.J.; methodology, J.C.; software, B.L.; validation, J.C. and B.L.; formal analysis, B.L.; investigation, B.L.; resources, F.J.; data curation, B.L.; writing—original draft preparation, J.C. and B.L.; writing—review and editing, F.J.; visualization, B.L.; supervision, J.C. and F.J.; project administration, F.J.; funding acquisition, F.J. All authors have read and agreed to the published version of the manuscript.

Funding: Financial support received from the Guangdong Science and Technology Department (2017B010120003, 2016A010104010, 2016A030313172, 2015A030308019), and the Guangzhou Scientific and Technological Development Plan (201804020020) is gratefully acknowledged.

Institutional Review Board Statement: Not applicable.

Informed Consent Statement: Not applicable.

Conflicts of Interest: The authors declare no conflict of interest.

References

1. Rao, Z.; Wang, S. A review of power battery thermal energy management. *Renew. Sustain. Energy Rev.* **2011**, *15*, 4554–4571. [[CrossRef](#)]
2. Wang, Q.; Sun, Q.; Ping, P.; Zhao, X.; Sun, J.; Lin, Z. Heat transfer in the dynamic cycling of lithium–titanate batteries. *Int. J. Heat Mass Transf.* **2016**, *93*, 896–905. [[CrossRef](#)]
3. Qian, L. A thermal-structure coupled optimization study of lithium-ion battery modules with mist cooling. *Int. J. Energy Res.* **2020**, *44*, 12295–12311. [[CrossRef](#)]
4. Wilke, S.; Schweitzer, B.; Khateeb, S.; Al-Hallaj, S. Preventing thermal runaway propagation in lithium ion battery packs using a phase change composite material: An experimental study. *J. Power Source* **2017**, *340*, 51–59. [[CrossRef](#)]
5. Wang, Q.; Ping, P.; Zhao, X.; Chu, G.; Sun, J.; Chen, C. Thermal runaway caused fire and explosion of lithium ion battery. *J. Power Source* **2012**, *208*, 210–224. [[CrossRef](#)]
6. Chiu, K.-C.; Lin, C.-H.; Yeh, S.-F.; Lin, Y.-H.; Huang, C.-S.; Chen, K.-C. Cycle life analysis of series connected lithium-ion batteries with temperature difference. *J. Power Source* **2014**, *263*, 75–84. [[CrossRef](#)]
7. Fleckenstein, M.; Bohlen, O.; Roscher, M.A.; Bäker, B. Current density and state of charge inhomogeneities in Li-ion battery cells with LiFePO₄ as cathode material due to temperature gradients. *J. Power Source* **2011**, *196*, 4769–4778. [[CrossRef](#)]
8. Zhao, R.; Zhang, S.; Liu, J.; Gu, J. A review of thermal performance improving methods of lithium ion battery: Electrode modification and thermal management system. *J. Power Source* **2015**, *299*, 557–577. [[CrossRef](#)]
9. Bandhauer, T.M.; Garimella, S.; Fuller, T.F. A critical review of thermal issues in Lithium-Ion batteries. *J. Electrochem. Soc.* **2011**, *158*, R1. [[CrossRef](#)]
10. Waldmann, T.; Wilka, M.; Kasper, M.; Fleischhammer, M.; Wohlfahrt-Mehrens, M. Temperature dependent ageing mechanisms in Lithium-ion batteries—A Post-Mortem study. *J. Power Source* **2014**, *262*, 129–135. [[CrossRef](#)]
11. Chung, Y.; Kim, M.S. Thermal analysis and pack level design of battery thermal management system with liquid cooling for electric vehicles. *Energy Convers. Manag.* **2019**, *196*, 105–116. [[CrossRef](#)]

12. Greco, A.; Jiang, X.; Cao, D. An investigation of lithium-ion battery thermal management using paraffin/porous-graphite-matrix composite. *J. Power Source* **2015**, *278*, 50–68. [[CrossRef](#)]
13. Panchal, S.; Khasow, R.; Dincer, I.; Agelin-Chaab, M.; Fraser, R.; Fowler, M. Thermal design and simulation of mini-channel cold plate for water cooled large sized prismatic lithium-ion battery. *Appl. Therm. Eng.* **2017**, *122*, 80–90. [[CrossRef](#)]
14. Lai, Y.; Wu, W.; Chen, K.; Wang, S.; Xin, C. A compact and lightweight liquid-cooled thermal management solution for cylindrical lithium-ion power battery pack. *Int. J. Heat Mass Transf.* **2019**, *144*, 118581. [[CrossRef](#)]
15. Chen, D.; Jiang, J.; Kim, G.-H.; Yang, C.; Pesaran, A. Comparison of different cooling methods for lithium ion battery cells. *Appl. Therm. Eng.* **2016**, *94*, 846–854. [[CrossRef](#)]
16. Temel, U.N. Passive thermal management of a simulated battery pack at different climate conditions. *Appl. Therm. Eng.* **2019**, *158*, 113796. [[CrossRef](#)]
17. Chen, F.; Huang, R.; Wang, C.; Yu, X.; Liu, H.; Wu, Q.; Qian, K.; Bhagat, R. Air and PCM cooling for battery thermal management considering battery cycle life. *Appl. Therm. Eng.* **2020**, *173*, 115154. [[CrossRef](#)]
18. Smith, J.; Singh, R.; Hinterberger, M.; Mochizuki, M. Battery thermal management system for electric vehicle using heat pipes. *Int. J. Therm. Sci.* **2018**, *134*, 517–529. [[CrossRef](#)]
19. Rao, Z.; Wang, S.; Wu, M.; Lin, Z.; Li, F. Experimental investigation on thermal management of electric vehicle battery with heat pipe. *Energy Convers. Manag.* **2013**, *65*, 92–97. [[CrossRef](#)]
20. Al-Zareer, M.; Dincer, I.; Rosen, M.A. Heat and mass transfer modeling and assessment of a new battery cooling system. *Int. J. Heat Mass Transf.* **2018**, *126*, 765–778. [[CrossRef](#)]
21. Wu, W.; Wang, S.; Wu, W.; Chen, K.; Hong, S.; Lai, Y. A critical review of battery thermal performance and liquid based battery thermal management. *Energy Convers. Manag.* **2019**, *182*, 262–281. [[CrossRef](#)]
22. Lu, M.; Zhang, X.; Ji, J.; Xu, X.; Zhang, Y. Research progress on power battery cooling technology for electric vehicles. *J. Energy Storage* **2020**, *27*, 101155. [[CrossRef](#)]
23. Liu, H.; Chika, E.; Zhao, J. Investigation into the effectiveness of nanofluids on the mini-channel thermal management for high power lithium ion battery. *Appl. Therm. Eng.* **2018**, *142*, 511–523. [[CrossRef](#)]
24. Zhang, W.; Liang, Z.; Wu, W.; Ling, G.; Ma, R. Design and optimization of a hybrid battery thermal management system for electric vehicle based on surrogate model. *Int. J. Heat Mass Transf.* **2021**, *174*, 121318. [[CrossRef](#)]
25. Bandhauer, T.M.; Garimella, S. Passive, internal thermal management system for batteries using microscale liquid–vapor phase change. *Appl. Therm. Eng.* **2013**, *61*, 756–769. [[CrossRef](#)]
26. Park, S.; Jang, D.S.; Lee, D.; Hong, S.H.; Kim, Y. Simulation on cooling performance characteristics of a refrigerant-cooled active thermal management system for lithium ion batteries. *Int. J. Heat Mass Transf.* **2019**, *135*, 131–141. [[CrossRef](#)]
27. Hong, S.H.; Jang, D.S.; Park, S.; Yun, S.; Kim, Y. Thermal performance of direct two-phase refrigerant cooling for lithium-ion batteries in electric vehicles. *Appl. Therm. Eng.* **2020**, *173*, 115213. [[CrossRef](#)]
28. Cen, J.; Li, Z.; Jiang, F. Experimental investigation on using the electric vehicle air conditioning system for lithium-ion battery thermal management. *Energy Sustain. Dev.* **2018**, *45*, 88–95. [[CrossRef](#)]
29. Kim, J.; Oh, J.; Lee, H. Review on battery thermal management system for electric vehicles. *Appl. Therm. Eng.* **2019**, *149*, 192–212. [[CrossRef](#)]
30. Hamut, H.S.; Dincer, I.; Naterer, G.F. Performance assessment of thermal management systems for electric and hybrid electric vehicles. *Int. J. Energy Res.* **2012**, *37*, 1–12. [[CrossRef](#)]
31. Hayes, J.G.; de Oliveira, R.P.R.; Vaughan, S.; Egan, M.G. Simplified electric vehicle power train models and range estimation. In Proceedings of the 2011 IEEE Vehicle Power and Propulsion Conference, Chicago, IL, USA, 6–9 September 2011; pp. 1–5.